



Supporting Online Material for

Constraints on the Formation Age of Cometary Material from the NASA Stardust Mission

J. E. P. Matzel,* H. A. Ishii, D. Joswiak, I. D. Hutcheon, J. P. Bradley, D. Brownlee,
P. K. Weber, N. Teslich, G. Matrajt, K. D. McKeegan, G. J. MacPherson

*To whom correspondence should be addressed. E-mail: matzel2@llnl.gov

Published 25 February 2010 on *Science Express*
DOI: 10.1126/science.1184741

This PDF file includes:

Materials and Methods

SOM Text

Figs. S1 to S3

Tables S1 to S3

References

SUPPORTING ONLINE MATERIAL

MATERIALS AND METHODS

Transmission Electron Microscopy – Focused Ion Beam Sample Preparation and Measurements

The Coki-5-B track was compressed, embedded in acrylic resin (1), and electron transparent thin-sections were prepared from the Coki particle using an ultramicrotome with a diamond knife at the University of Washington. Sections 50-80 nm in thickness were mounted on continuous carbon substrates supported on 3 mm diameter Cu-mesh grids. The thin sections were examined using transmission electron microscopy, and mineral compositions (Table S1, Fig. S1) were determined by energy dispersive x-ray spectroscopy (EDS). Microscopes used in this work are two 200kV FEI Tecnai F20 field-emission scanning transmission electron microscopes ((S)TEM) each with a Gatan energy filter, EDAX Si(Li) solid state energy-dispersive X-ray detector and high angle annular dark field (HAADF) detector at the University of Washington and at Lawrence Livermore National Laboratory. Bright-field, dark-field imaging, diffraction, tilting experiments and EDS were used to locate and identify minerals present including (Mg-rich) spinel inclusions <200 nm in diameter. Mineral maps were produced by examining samples shard-by-shard using conventional TEM-EDS rather than by (S)TEM x-ray mapping to minimize any potential effects of electron beam damage.

After TEM characterization of Coki, an FEI Nova NanoLab 600 dual-beam focused ion beam (FIB) instrument at Lawrence Livermore National Laboratory was used to deposit ~10 µm wide and ~1 µm thick Pt ribbons behind the sample by interaction of first the electron, and then the ion, beam with a locally-injected organometallic gas. The Pt provides a conductive mechanical support allowing the fragile ultramicrotomed section to undergo NanoSIMS analysis. After back-coating the sample, a JEOL JSM-5800 LV secondary electron microscope (SEM) was used to generate high resolution images for correlation of Coki fragment topography with the TEM mineral map in order to identify pyroxene and

spinel locations. The 30 kV Ga⁺ ion beam of the FIB instrument was then used to precisely and accurately mill away submicron-sized pyroxene fragments with a current of 30 pA (Figs. 1 and S2). The pyroxene was removed to mitigate dilution of the anorthite Mg isotopic signature by the surrounding pyroxene (2).

NanoSIMS Measurements

Isotope measurements were made by rastering a 3 pA O⁻ primary ion beam focused to a ~200 nm diameter spot over sample areas ranging in size from 2 x 2 μm² to 3 x 3 μm² until the sample was consumed. Images consist of up to 600 replicate scans of 32² pixels with a dwell time of 10 ms/pixel. Four ion images were simultaneously collected on electron multipliers corresponding to ²⁴Mg⁺, ²⁵Mg⁺, ²⁶Mg⁺ and ²⁷Al⁺ secondary ions. A mass resolving power of ~3700 was used to separate hydride or other interferences from the isotopes of interest.

Instrumental mass fractionation was accounted for by comparing the measured ²⁵Mg/²⁴Mg ratio of mineral standards with the ²⁵Mg/²⁴Mg of terrestrial Mg (0.12663, 3) and is given in parts per thousand (permil, ‰) per amu by

$$\Delta^{25}\text{Mg} = [\{ ({}^{25}\text{Mg}/{}^{24}\text{Mg})_{\text{meas}} / 0.12663 \} - 1] \times 1000.$$

Standards analyzed in this study include Burma spinel, Miakejima plagioclase, and a synthetic anorthite composition glass. These standards provide a test of the NanoSIMS measurement because they have a range of Al/Mg concentrations and no radiogenic ²⁶Mg, and therefore they yield the same ²⁶Mg/²⁴Mg ratio relative to Al/Mg ratio. After correcting for instrumental mass fractionation using a linear law, the weighted average ²⁶Mg/²⁴Mg ratio of all terrestrial materials was 0.14227 ± 0.00012 (Table S2). The measured average ²⁶Mg/²⁴Mg is higher than the reference value of terrestrial Mg (0.13932, 3) presumably because of differences in the gain between detectors. Any potential excess ²⁶Mg that

remained after correcting for mass fractionation is reported in permil relative to the measured $^{26}\text{Mg}/^{24}\text{Mg}$ of our standards:

$$\delta^{26}\text{Mg} = [\{ (^{26}\text{Mg}/^{24}\text{Mg})_{\text{meas}} / 0.14227 \} - 1] \times 1000.$$

The two analyses of Miakejima plagioclase were obtained from small (<3 μm) fragments that had been prepared in a manner identical to the Coki thin section. These analyses demonstrate that sample preparation did not bias the results.

Potential differences in ionization efficiency between Al and Mg were addressed by comparing the measured $^{27}\text{Al}^+ / ^{24}\text{Mg}^+$ to the “true” $^{27}\text{Al} / ^{24}\text{Mg}$ of the anorthite composition. No correction to the measured $^{27}\text{Al}^+ / ^{24}\text{Mg}^+$ ratio was necessary.

We also analyzed two suites of isotopically-enriched synthetic glasses to test our ability to precisely and accurately measure deviations from the normal isotopic composition not due to mass dependent fractionation. These suites include two anorthite composition glass standards spiked with varying amounts of ^{25}Mg (4) and three pyroxene composition glass standards spiked with ^{26}Mg (K. McKeegan, unpublished data). The results from each standard agree well with gravimetrically calculated values (Table S3).

The Coki and Miakejima plagioclase data were processed as quantitative isotope ratio images using custom software (LIMAGE, L.R. Nittler). Each image was subdivided into regions based on the $^{27}\text{Al} / ^{24}\text{Mg}$ ratio of individual pixels. The subdivision resulted in three spatially continuous regions (Fig. S3) corresponding to the three Coki data points in figure 3. The isotopic composition of each region was calculated by dividing the total counts of each isotope species in a given region and averaging the ratios over all of the replicate scans and all of the images. The reported error on the ratios is the 2σ standard error of the mean or the 2σ error based on counting statistics, whichever is larger.

MINERALOGY OF TRACK 141

Track #141 is a 2 mm long, type B track (5). The refractory particle, Coki, was one of the more competent and coarse fragments found along with two pyroxene fragments, an $\sim 3 \mu\text{m}$ in diameter aggregate of Fe-rich olivine, augite and albite or albitic glass, and the terminal particle in the track, a $\sim 5 \mu\text{m}$ in diameter pentlandite fragment with attached Fe-rich olivine and augite and glass. The bulbous, upper track contained the only identified presolar silicon carbide crystal in the Stardust materials (6-7). The genetic relationship between the fragments, if any, is unclear.

The possibility that Coki did not originate from Comet Wild 2, but was rather a passing interplanetary dust particle (IDP), is highly unlikely for several reasons. 1) CAI-like objects are very rare in IDPs. 2) There were no impacts of the size of the particle that generated track #141 on the interstellar side of the collector which supports our assertion that impacts from IDPs are very rare events. 3) Impacts from passing IDPs would be expected to produce randomly oriented tracks. However, no off-normal tracks were observed on the cometary side of the collector, and off-normal tracks seen on the interstellar side of the collector have been shown to have been produced by secondary debris from an impact with the spacecraft.

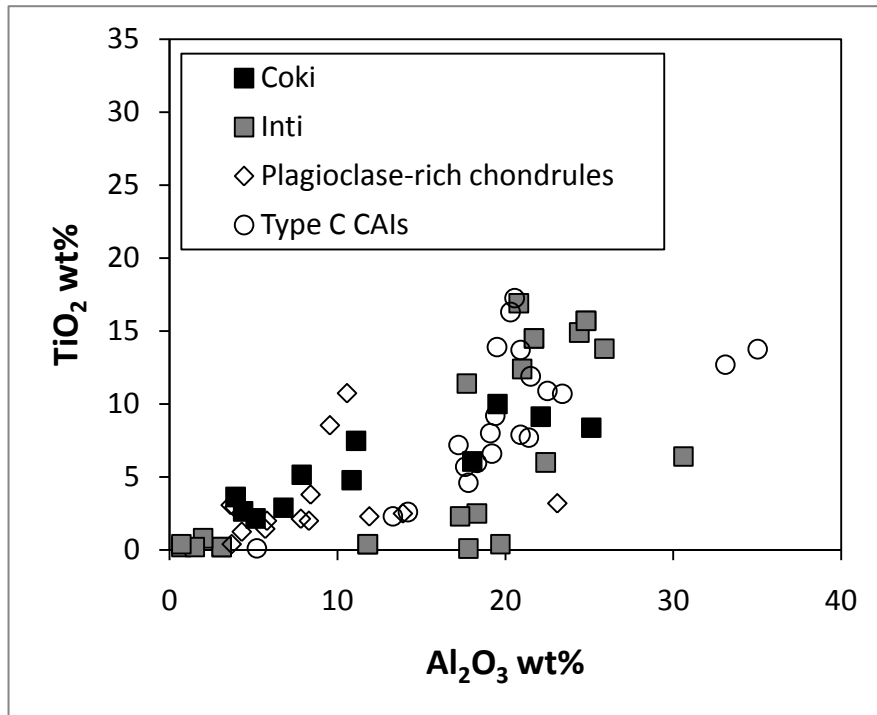


Figure S1. Coki pyroxene compositions as compared to type C CAIs (8-9), plagioclase-rich chondrules (8, 10-11), and Inti (12). Coki pyroxene compositions are Ca-, Al-, and Ti-rich relative to chondrule pyroxene compositions.

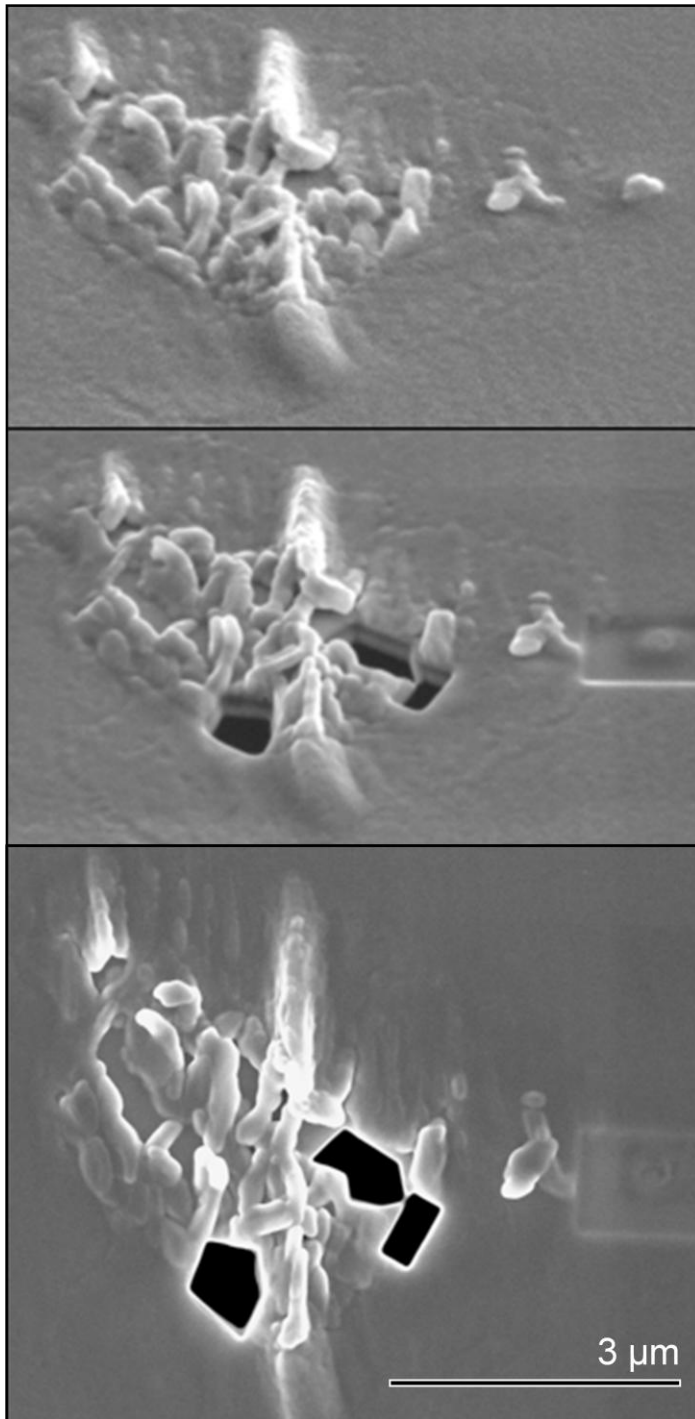


Figure S2. Removal of pyroxene fragments to mitigate dilution of anorthite Mg isotope signatures. Secondary electron images of the Coki particle thin section (top) at a tilt of 52° prior to any focused ion beam milling and (middle) at a tilt of 52° and (bottom) 0° after focused ion beam milling of selected pyroxene fragments. A rectangular region at the right containing a fragment of Na-augite was imaged by the ion beam for the purpose of focus and stigmatism of the beam prior to milling.

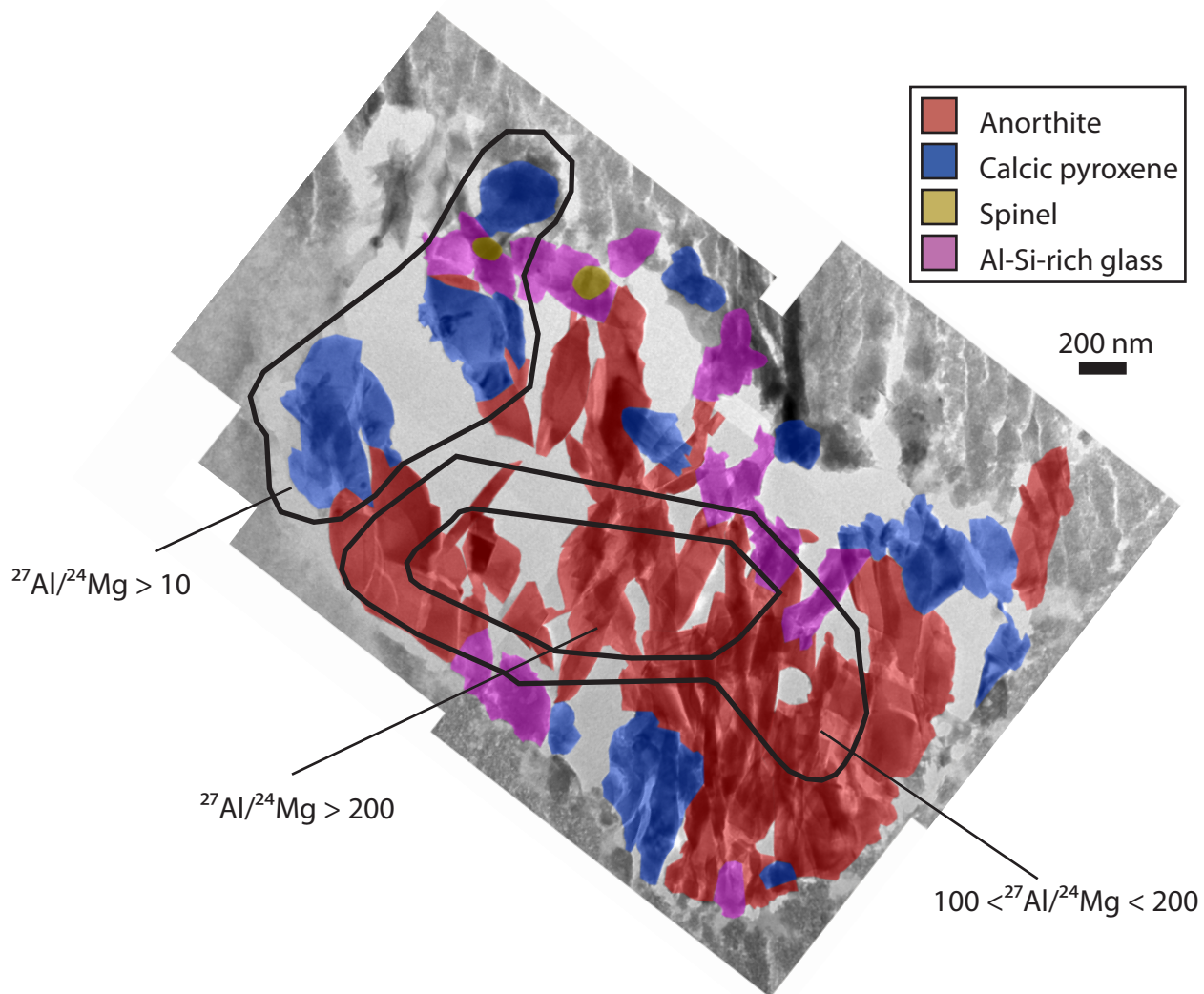


Figure S3. False color mineral map of the Coki section overlaid on a montage of brightfield TEM images. Heavy black lines outline the regions incorporated into each data point.

Table S1. Chemical compositions of Coki pyroxene and anorthite determined by TEM/EDS.

Mineral	pyroxene											anorthite			
	Spot Number	UW -1	UW -2	UW -3	UW -4	UW -5	UW -6	LLNL -1	LLNL -2	LLNL -3	LLNL -4	LLNL -5	LLNL -1	LLNL -2	LLNL -3
SiO ₂		37.6	56.1	54.6	45.6	45.7	45.0	43.9	41.8	53.7	40.9	50.3	41.7	43.2	41.8
TiO ₂		10.0	2.6	3.6	5.2	4.8	7.5	9.1	6.1	2.2	8.4	2.9	n.m.	n.m.	n.m.
Al ₂ O ₃		19.5	4.4	3.9	7.9	10.8	11.1	22.1	18.0	5.1	25.1	6.8	37.0	36.7	38.9
Cr ₂ O ₃		0.1	n.d.	0.2	0.3	0.3	n.d.	n.d.	n.d.	n.d.	0.4	0.2	n.m.	n.m.	n.m.
FeO		n.d.	0.3	0.2	0.4	0.3	0.2	n.d.	n.d.	n.d.	n.d.	n.d.	n.m.	n.m.	n.m.
V ₂ O ₃		n.d.	n.d.	n.d.	0.2	0.3	0.3	n.m.	n.m.	n.m.	n.m.	n.m.	n.m.	n.m.	n.m.
MgO		8.4	16.4	15.4	16.4	14.1	12.5	6.9	10.0	20.0	8.4	16.1	n.m.	n.m.	n.m.
CaO		24.4	20.2	22.0	24.0	23.6	23.4	18.0	24.2	19.0	16.6	23.5	21.3	20.2	19.3

Analyses are normalized to 100 wt% oxides. Relative uncertainties (1 σ) based on counting statistics are <5% for SiO₂, Al₂O₃, MgO, CaO <15% for TiO₂, and <30% for V₂O₃, Cr₂O₃, and FeO. n.m.: not measured; n.d.: not detected

Table S2. Isotope data from terrestrial standards.

Standard	n [†]	²⁵ Mg/ ²⁴ Mg [‡]	²⁶ Mg/ ²⁴ Mg [‡]	²⁷ Al/ ²⁴ Mg
Anorthite glass	6	0.12390 ± 0.00026	0.14325 ± 0.00061	108 ± 4.4
Miakejima plagioclase	2	0.12367 ± 0.00086	0.14291 ± 0.00191	340 ± 24
Burma spinel	8	0.12445 ± 0.00005	0.14223 ± 0.00012	2.0 ± 0.1
Weighted mean			0.14227 ± 0.00012	

[†]Number of analyses

[‡]Mean and 2 σ uncertainty of n measurements.

[‡]Fractionation corrected ²⁶Mg/²⁴Mg (assuming linear fractionation law and ²⁵Mg/²⁴Mg = 0.12663).

Uncertainties are 2 σ .

Table S3. Mg isotope data from isotopically enriched standards.

Standard	n [†]	δ ²⁶ Mg (‰) [‡]	δ ²⁶ Mg (‰) by gravimetry	δ ²⁵ Mg (‰) [¥]	δ ²⁵ Mg (‰) by gravimetry
P0	6	0.0 ±0.7	0.0	–	–
P10	3	10 ±0.9	10.05	–	–
P99	3	99 ±1.1	99.0	–	–
AnMg-6	1	–	–	9.5 ±6.0	9.4
AnMg-8	1	–	–	97 ±8.2	97.9

[†]Number of analyses

[‡]²⁶Mg-enrichment after correcting for mass fractionation (assuming linear fractionation law and ²⁵Mg/²⁴Mg = 0.12663) reported in permil relative to terrestrial Mg.

[¥]²⁵Mg-enrichment after correcting for mass fractionation (assuming linear fractionation law and ²⁶Mg/²⁴Mg = 0.13932) reported in permil relative to terrestrial Mg.

REFERENCES

1. G. Matrajt, D. E. Brownlee, *Meteoritics & Planet. Sci.* **41**, 1715 (2006).
2. H. A. Ishii *et al.*, *Proceedings of the Lunar and Planetary Science Conference* **40**, 2288 (2009).
3. E. Catanzaro, T. Murphy, E. Garner, W. Shields, *Journal of Research of the National Bureau of Standards* **70A**, 453 (1966).
4. J. T. Armstrong, J. C. Huneke, H. F. Shaw, T. A. Finnerty, G. J. Wasserburg, in *Microbeam Analysis - 1982*, K. F. J. Heinrich, Ed. (San Francisco Press, San Francisco, 1982), pp. 205-209.
5. F. Hörz *et al.*, *Science* **314**, 1716 (2006).
6. D. E. Brownlee, D. Joswiak, G. Matrajt, S. Messenger, M. Ito, in *Lunar and Planetary Institute Science Conference Abstracts*. (2009), vol. 40, pp. 2195.
7. S. Messenger, D. Joswiak, M. Ito, G. Matrajt, D. E. Brownlee, in *Lunar and Planetary Institute Science Conference Abstracts*. (2009), vol. 40, pp. 1790.
8. A. N. Krot *et al.*, *Geochim. Cosmochim. Acta* **71**, 4342 (2007).
9. D. A. Wark, *Geochim. Cosmochim. Acta* **51**, 221 (1987).
10. G. J. MacPherson, G. R. Huss, *Geochim. Cosmochim. Acta* **69**, 3099 (2005).
11. Y. J. Sheng, I. D. Hutcheon, G. J. Wasserburg, *Geochim. Cosmochim. Acta* **55**, 581 (1991).
12. S. B. Simon *et al.*, *Meteoritics & Planet. Sci.* **43**, 1861 (2008).